

# SIMULATION STUDY OF THE EFFECT OF THE PROTON LAYER THICKNESS ON TNSA

Z. Lecz, O. Boine-Frankenheim, TU Darmstadt and GSI Darmstadt, Germany  
V. Kornilov, GSI, Darmstadt, Germany

## INTRODUCTION

The LIGHT project at GSI is a collaboration of several laser and accelerator laboratories in Germany with the purpose to consolidate the theoretical, numerical and experimental investigations for the usage of laser accelerated ions in conventional accelerators. The acceleration of ions with lasers up to energies of 60 MeV has been successfully demonstrated at different laser systems worldwide, including our facility: PHELIX [1]. The undergoing mechanism is understood as Target Normal Sheath Acceleration (TNSA) [2]. Due to the small transverse emittance and low installation cost laser-ion acceleration is a promising alternative to RF accelerators with the possible application in ion cancer therapy [3]. This contribution is devoted to the numerical investigation of the proton acceleration via the TNSA mechanism using 1D and 2D particle-in-cell electro-magnetic simulations. We employ the plasma simulation code VORPAL [4] and focus on the proton and electron phase-space distribution at the rear side of the target. The lack of knowledge about the thickness of hydrogen-rich contamination layer requires a detailed parameter study. In this work we investigate the regime between two already well-understood mechanisms: quasi-static acceleration [5, 6] and isothermal expansion [7, 8].

## DEBYE-SHEATH FORMATION ON THE TARGET SURFACE

The initial target foil consists of heavy ions (they are considered immobile), protons, cold and hot electrons. Heavier light ions, like oxygen, carbon, we neglect in this study. Due to their high energy the hot electrons can escape from the target and build up a stable electric field, which has an exact form outside, close to the plasma surface [9]:

$$E(x) = 2E_0 / (\sqrt{2 \exp(-\varphi_0)} + \frac{x}{\lambda_D}) \quad (1)$$

where  $E_0 = \sqrt{n_{h0} T_h / \epsilon_0}$  is the self-similar electric field,  $\lambda_D = (\epsilon_0 T_h / (e n_{h0}))^{1/2}$  is the hot electron Debye-length and  $n_{h0}$ ,  $T_h$  are the hot electron density and temperature inside the plasma. The corresponding potential is just the integral of  $E$ :

$$\varphi(x) = \varphi_0 - 2 \ln \left( 1 + \frac{x}{\lambda_D \sqrt{2 \exp(-\varphi_0)}} \right) \quad (2)$$

The potential is normalized to  $T_h/e$ ,  $e$  is the elementary charge, and at the plasma surface,  $\varphi_0 = \varphi(x=0)$ , it has the following value [9]:

$$\varphi_0 = - \frac{1 + (n_{c0}/n_{h0})(T_c/T_h)}{1 + n_{c0}/n_{h0}} \quad (3)$$

where  $n_{c0}$ ,  $T_c$  are the cold electron density and temperature. The value of  $\varphi_0$  is  $-1$  when the cold electron density is zero (one-temperature plasma) and  $\approx 0$  when the cold electron population becomes dominant. Usually the latter is the case in the interaction of laser with overdense plasma.

Inside of the plasma,  $x < 0$ , the potential can not be calculated analytically, but a mathematical approximation suggests that it should be an exponential function of  $x$  [9]:

$$\varphi_{in}(x) \approx \varphi_0 \exp(rx/\lambda_D) \quad (4)$$

where  $r = \sqrt{1 + (n_{c0}/n_{h0})(T_h/T_c)}$ . In our simulations this expression is used to get an analytical expression for the hot and cold electron density. It is needed to obtain an initial thermal equilibrium for the electrons, which would be achieved only after many plasma oscillations, if we used a step-like density profile.

## INITIAL CONDITIONS FOR THE SIMULATION

We assume that the electrons have a Boltzmann distribution:  $n_e(x) = n_{h0} \exp(\varphi(x))$ . Outside of the plasma,  $x > 0$ , only hot electrons are present, therefore their density profile is trivial:

$$n_h(x) = n_{h0} \frac{2}{(\sqrt{2e^{-\varphi_0}} + x/\lambda_D)^2} \quad (5)$$

The extension of the electron cloud depends on the maximum electron energy ( $\epsilon_{max}$ ) and the correct shape of the potential far from the target can not be calculated analytically [5]. In our simulations we use the profile Eq. 5 and we define the end of the electron cloud as the point where the potential is equal to  $\epsilon_{max}$ :

$$L_e = \lambda_D \sqrt{2 \exp(-\varphi_0)} \left( \exp \left( \frac{\varphi_0 + \epsilon_{max}}{2T_h} \right) - 1 \right) \quad (6)$$

For  $\epsilon_{max}$  we choose  $7.5T_h$ , it is a parameter which can be varied and the initial Maxwellian velocity distribution of electrons has to be truncated according to this cut-off energy. This value is close to the prediction of scaling laws used by Passoni [6] if we use the laser parameters of PHELIX at GSI. A higher value of  $\epsilon_{max}$  would require longer simulation box, which means more CPU time for simulations.

Inside of the plasma,  $x < 0$ , in the one-temperature (1T) case the hot electron density is approximated using Eq. 4:

$$n_h(x) = n_{h0} \exp(\varphi_0 \exp(\alpha r \sqrt{2 \exp(\varphi_0)} x / \lambda_D)) \quad (7)$$

where  $\alpha$  must be calculated from the neutrality condition, the total charge is zero in the system, and  $r = 1$ . In the two-temperature (2T) plasma the cold electrons dominate inside of the plasma, therefore for their density we use Eq. 7, but the potential is normalized by the cold temperature and for the hot electrons we use a similar exponential function, obeying the correct boundary conditions for the electric field:

$$n_h(x) = n_{h0} \exp\left(\frac{\varphi_0}{r} \exp\left(\frac{r}{\varphi_0} \sqrt{2 \exp(\varphi_0)x/\lambda_D}\right)\right) \quad (8)$$

In this way we can simulate a correct charge separation at a plasma surface including one- or two-temperature electrons, which are in thermal equilibrium.

The protons are initially placed in the interval  $x = [-d, 0]$ , where  $d$  is the layer thickness. The simulation parameters which we used: the total plasma length  $L_p/\lambda_D = 20$  in 1T and 4 in 2T simulation,  $n_{c0}/n_{h0} = 3$ ,  $T_c/T_h = 0.05$ . The heavy ions are placed in the interval  $[-L_p, -d]$ . Numerical parameters: grid size  $dx = \lambda_{Dc}/10$ , where  $\lambda_{Dc} = (\epsilon_0 T_c / (en_0))^{1/2}$ ,  $n_0 = n_{c0} + n_{h0}$ , in the 1T case  $T_c = T_h$  and  $n_{c0} = 0$ . Time step:  $dt = 0.9dx/c$ , where  $c$  is the speed of light and the number of macro-particles per cell is 1000. The plasma density is  $n_0 = 10^{28} \text{ m}^{-3}$  and the hot electron temperature is  $T_h = 10^4 \text{ eV}$ .

## QUASI-STATIC ACCELERATION VS. ISOTHERMAL EXPANSION

As we have seen the electric field inside the has an exponential form with a scale length equal to  $\lambda_D/r$ . Therefore we introduce the dimensionless layer thickness,

$$D = r \frac{d}{\lambda_D} = \sqrt{1 + \frac{n_{c0} T_h}{n_{h0} T_c}} \frac{d}{\lambda_D} \quad (9)$$

Let us consider a layer thickness much thinner than the penetration depth of the electric field into the target. In this case the protons are accelerated as test particles, all of them feel the same field strength and finally they form a quasi-mono-energetic bunch with energy  $W_{qsa} = \epsilon_{max} - 1$  [5, 6]. In our case  $W_{qsa} \approx 6.5$ , but in reality it depends on the fast electron generation during the laser-plasma interaction. The corresponding velocity we can estimate as

$$v_{max} = 2C_s \sqrt{\ln(1 + L_e / (\lambda_D \sqrt{2e^{-\varphi_0}}))} \quad (10)$$

where  $C_s = \sqrt{T_h/m_p}$ ,  $m_p$  is the proton mass.

In the opposite extreme case, when  $D \gg 1$ , the protons are accelerated via isothermal expansion [7], which can be described analytically up to the point when the adiabatic phase starts (the electron cooling is important) [8]. This time is approximately the laser pulse duration, but in the case of an expanding plasma slab the acceleration time is  $t_{acc} \approx d/C_s$ . The final velocity can be estimated using the following formula:

$$v_f = 2C_s \ln\left(\tau + \sqrt{1 + \tau^2}\right) \quad (11)$$

where  $\tau = \omega_{pi} t / \sqrt{2e^{-\varphi_0}}$ ,  $\omega_{pi} = \sqrt{\frac{n_{h0} q_e^2}{m_p \epsilon_0}}$  and  $q_e$  is the elementary charge.

In Fig. 1 we compare two extreme cases: mono-layer of protons ( $D = 0.01$ ) accelerated in the constant electric field achieving the final velocity Eq. 10, which gives  $\approx 3.7C_s$ . The thick proton layer,  $D = 10$ , expands isothermally and the front velocity, presented by the black line, agrees with Eq. 11 for  $\omega_{pi} t_{acc} \approx 10$ .

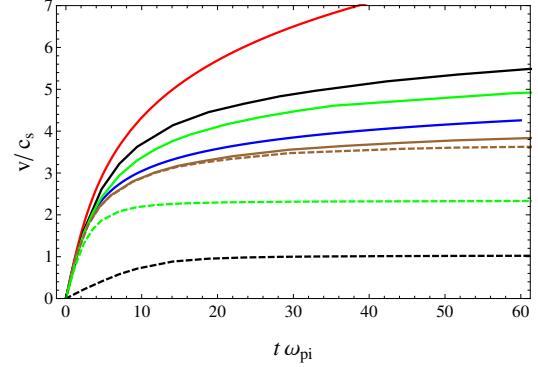


Figure 1: Maximum velocity of protons for  $D = 0.01$  (—),  $0.5$  (—),  $10$  (—) and mean velocity (dashed lines). The blue line is the solution of equation of motion in the field represented by Eq. 1. The red full line is given by Eq. 11.

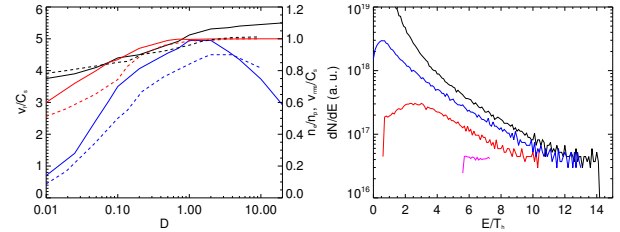


Figure 2: Left: Front velocity of the protons (black), neutrality factor (red) defined as  $n_e/n_p$  in the bunch and RMS velocity (blue) at  $\omega_{pi} t = 60$  for 1T (full) and 2T (dashed) plasma. Right: Final energy spectra of protons for  $D = 0.01$  (pink),  $0.2$  (red),  $1$  (blue) and  $10$  (black).

## INTERMEDIATE LAYER THICKNESS

The acceleration in the intermediate regime can not be described analytically. The simulation results are represented as a function of dimensionless layer thickness in Fig. 1 and 2. There is a smooth transition between the two models discussed in the previous section. In the case of a very thin layer the accelerated protons form a quasi-monoenergetic beam (pink line in Fig. 2, right) and in the case of thick layer (black line) the spectrum is similar to an exponential energy distribution [7].

For intermediate thicknesses the proton bunch detaches from the target and gets accelerated in the static field until it reaches the position  $x_t$ . In Fig. 3, left we can see that a bump appears in the potential (black curve) and the

electron trapping starts. Later the proton bunch expands and due to the trapped neutralizing electrons the potential takes a constant value along the bunch, like in the case of blue curve, but there the trapping started earlier. Thus between the plasma surface and bunch tail evolves a potential-drop ( $\phi_d$ ). If we assume that the potential profile does not change significantly before the electron trapping,  $\phi_d$  can be calculated using Eq. 2:  $\phi_d = -\varphi(x_t(d))$  and it can be fitted with the following function:  $x_t(d) = a + b/(d + c)$ , where  $a, b, c$  are constants. A good fit can be seen in Fig. 3, right, with parameters:  $a = -0.4, b = 1.8, c = 0.025$ . For thick layers the potential-drop converges to  $-\varphi_0$ .

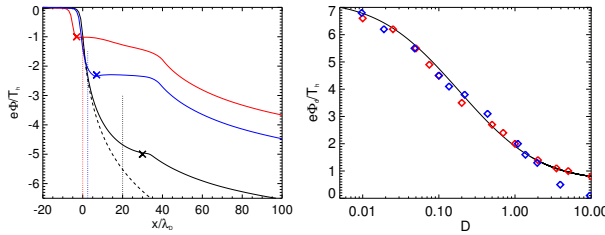


Figure 3: Left: Modified potential profiles at  $\omega_{pi}t = 14$  in 1T plasma for  $d = 0.05\lambda_D$  (black),  $0.9\lambda_D$  (blue),  $5\lambda_D$  (red). The dashed line shows the initial profile (Eq. 2) and the vertical lines indicate  $x_t$ . The “x” marks show the position of the bunch tail. Right: Potential drop measured from 1T (red) and 2T (blue) simulations, the best fit (black full line) with a fitting function.

Mostly the electrons with a kinetic energy higher than  $\phi_d$  contribute to the acceleration, which is confirmed in Fig. 4, left. By integrating the Maxwellian energy distribution of electrons from  $\phi_d$  until  $\epsilon_{max}$  and dividing by the total initial electron energy we obtain the energy conversion from the electrons to the protons as a function of  $D$ :

$$W_p = \frac{2}{T_h} \int_{e\phi_d}^{\epsilon_{max}} E f_e(E) dE \quad (12)$$

where  $f_e(E) = (\sqrt{2\pi T_h E})^{-1} \exp(-E/T_h)$ . This expression is independent of the plasma, because  $\phi_d$  is the same in 1T and 2T plasma, this is why we show only one blue line in Fig. 4, right. The red lines represent the QSA regime:

$$W_p = 2(\epsilon_{max} - 1) \frac{n_p}{n_{h0}} \frac{d}{L_p} \quad (13)$$

The energy conversion is better in the 2T case because the total electron energy is smaller. In Fig. 4 the analytical prediction Eq. 13 is correct in the small  $D$  regime, while Eq. 12 agrees with the simulation only in the 1T case for large  $D$  values, because in the 2T case  $\phi_d$  goes to zero, but our fit does not. The smaller the  $\phi_d$  the more energy is given to the protons, but the maximum velocity does not increase significantly, as it is shown in Fig. 1, right. In the isothermal expansion [7] the number of high energy protons is very small so the mean velocity is decreasing with increasing the layer thickness. For a mono-layer the mean

velocity is almost equal to the maximum velocity, which means no energy spread.

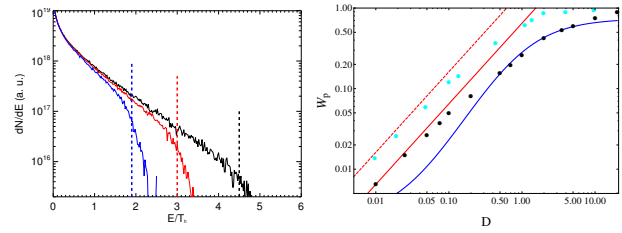


Figure 4: Left: Electron spectra at the end of acceleration for  $D = 0.1$  (black),  $0.22$  (red) and  $1$  (blue). The dashed lines indicate the corresponding potential-drops. Right: Final proton energy over the initial total energy of electrons. Simulation results are presented in 1T (black dots) and 2T (cyan) case. The blue line represents Eq. 12 and the red lines show Eq. 13 for 1T (full) and 2T (dashed) plasma.

As we can see in Eq. 12 the energy conversion for thick layers does not depend on the plasma thickness (or laser pulse duration). For thick layers the total proton energy depends on the pulse duration, but for very thin layers a short pulse is sufficient to gain the maximum energy ( $W_{qsa}$ ).

## CONCLUSIONS

The TNSA in the intermediate regime with respect to the layer thickness has been studied including only protons in the contamination layer on the target surface. By performing a detailed parameter-scan using the VORPAL PIC plasma simulation code we could describe the basic energy conversion mechanism from electrons to the protons. The potential drop  $\phi_d$  has been fitted with an analytical curve. In the two extreme cases, QSA and isothermal expansion, the proton front velocity has been compared with analytical predictions. Two important parameters determine the proton cut-off energy: maximum electron energy in the QSA regime and laser pulse duration in the isothermal expansion.

## REFERENCES

- [1] <http://www.gsi.de/forschung/pp/phelix/>
- [2] S. C. Wilks et al., Phys. Rev. Lett., **69**, 1383 (1992)
- [3] I. Hofmann, et al., PRST-AB, **14**, 31304 (2011)
- [4] <http://www.txcorp.com/products/VORPAL/>
- [5] M. Passoni et al., Phys. of Plasmas, **13**, 042102 (2006)
- [6] M. Passoni et al., Phys. Rev. Lett., **101**, 115001 (2008)
- [7] P. Mora, Phys. Rev. Lett., **90**, 185002 (2003)
- [8] P. Mora, Phys. Rev. E, **72**, 056401 (2005)
- [9] M. Passoni et al., Phys. Rev. E, **69**, 026411 (2004)